The Ever-Elusive Blowup in the Mathematical Description of Fluids

Robert M. Kerr and Marcel Oliver

Abstract. This contribution introduces you to the Euler equations of ideal fluids and the Navier–Stokes equations which govern fully developed turbulent flows. We describe some of the unresolved mathematical issues, including the "Navier–Stokes millennium problem", and the role numerical simulations play in developing this field.

1 Introduction

When you think of turbulence, you might recall the jostling and vibrations during a recent flight. Or maybe the irregular turning and twisting motions surrounding a hurricane or storm. But you don't need to look far to feel, if not see, a turbulent flow. The truth is that turbulence surrounds us almost all the time. It explains how heat and cold can quickly fill the room you are in, even if breezes are kept out. Turbulence around wings is essential for explaining the flight of airplanes and gliders. And this mundane turbulence is even less understood than the large vortices and waves primarily responsible for clear air turbulence during flight or the strong shears during storms.

Part of the reason is that, while the equations we use to represent and simulate fluids have been known for almost 200 years, we do not know whether they meet fundamental mathematical criteria. In particular,

Robert M. Kerr
Department of Mathematics, School of Engineering, and Centre for Scientific Computing, University of Warwick, Gibbet Hill Road, Coventry CV4 7AL, UK.
e-mail: Robert.Kerr@warwick.ac.uk

Marcel Oliver
School of Engineering and Science, Jacobs University, 28759 Bremen, Germany.
e-mail: oliver@member.ams.org

could solutions to these equations develop discontinuities or singularities? If they do, our description of small scale flow must be missing essential physics.

This contribution aims at introducing the underlying mathematical problem in simple, yet precise terms and link it to insight that could be gained from computer simulation. We begin by introducing the incompressible Euler and Navier–Stokes equations of fluid dynamics. Section 3 explains conservation laws which provide important structural information. Section 4 introduces the open mathematical question of global regularity of solutions, while Section 5 sketches some heuristics which shape our current understanding. Sections 6 and 7 look at the interplay between theory and numerical experiment for guiding our choice of initial conditions and validating the results of a simulation. The final Section 8 looks into the future, sketching out new directions for research.

The article is supplemented by three more technical appendices. For readers who might not be comfortable with multivariable calculus, Appendix A introduces the main concepts and formulas in an intuitive, yet concise fashion. Appendix B explains so-called energy estimates, which give a caricature of what is known about the Navier–Stokes equations. Finally, Appendix C sketches some of the concepts behind spectral and pseudo-spectral numerical methods.

Giving complete and proper attribution is beyond what we can hope to achieve in the format of this contribution. Thus, we make no serious attempt to cite original research papers, but hope that the enterprising reader will look at the excellent recent review articles [2, 4, 5, 6, 9, 10, 12, 15, 17] and, from there, venture further into the vast body of specialized literature.

2 The Equations of Fluid Mechanics

Equations governing fluid motion may, at first glance, look intimidating. The underlying principles, however, are surprisingly simple: we apply Newton's second law of mechanics in a continuum setting and make assumptions on the mechanical forces that characterize a fluid.

Newton's equation $\boldsymbol{F} = m\boldsymbol{a}$, which says that the mechanical force on a point-particle equals its mass times its acceleration, will look familiar to anyone with some background in high school physics. Using calculus, we introduce the instantaneous velocity $\boldsymbol{v}(t)$ as the time derivative of position $\boldsymbol{x}(t)$ and the instantaneous acceleration $\boldsymbol{a}(t)$ as the time derivative of velocity $\boldsymbol{v}(t)$. When the force is a known function of position, Newton's law leads to the differential equation $\boldsymbol{F}(\boldsymbol{x}(t)) = m\,\mathrm{d}^2\boldsymbol{x}(t)/\mathrm{d}t^2$, where the particle trajectory $\boldsymbol{x}(t)$ is an unknown function to be solved for.

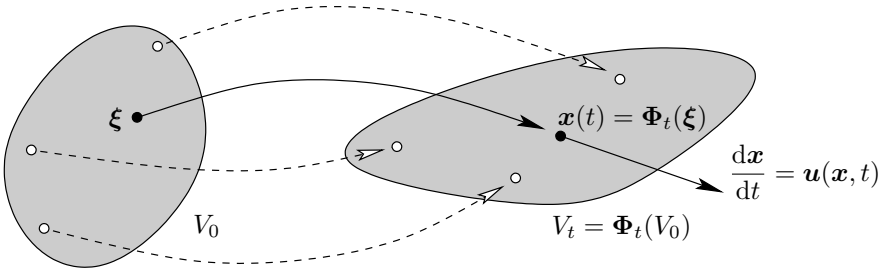

Fig. 1. The flow map $\boldsymbol{\Phi}_t$ maps the initial configuration of the fluid to its configuration at a later time $t > 0$, thereby deforming an original sub-volume V_0 into V_t. A distinguished "fluid particle" at initial location $\boldsymbol{\xi}$ is transported to location $\boldsymbol{x}(t) = \boldsymbol{\Phi}_t(\boldsymbol{\xi})$ where it moves with velocity $\boldsymbol{u}(\boldsymbol{x}(t), t) = \mathrm{d}\boldsymbol{x}/\mathrm{d}t$.

A fluid can be seen as a continuum of particles: consider some container (or *domain*) $\Omega \subset \mathbb{R}^d$ in $d = 2$ or $d = 3$ space dimensions entirely filled with point-particles. Pick a particle at location $\boldsymbol{\xi} \in \Omega$ at time $t = 0$, and denote its trajectory by $\boldsymbol{x}(t)$. There will be exactly one such trajectory emanating from every point in Ω. Therefore, the collection of trajectories defines, for each fixed time t, a mapping $\boldsymbol{\Phi}_t$ from the domain Ω into itself; see Figure 1. This mapping is referred to as the *flow map*.

Newton's law now applies to each fluid particle; more precisely, it applies to the fluid contained in each sub-volume V_t in the limit that the size of the sub-volume goes to zero. In this limit, Newton's law equates forces per volume. In particular, mass m is replaced by *mass density* $\rho(\boldsymbol{x}, t)$, the mass per volume,[1] so that Newton's law states that $\rho\boldsymbol{a}$ equals force per volume.

The setting so far applies to any type of mechanical continuum. A fluid, in particular, is characterized by the assumption that each particle pushes its neighbors equally in every direction. Then, a single scalar quantity $p(\boldsymbol{x}, t)$, the *pressure*, describes the force per area that a particle at location $\boldsymbol{x} \in \Omega$ exerts on all its neighbors at time t. A particle is not accelerated if its neighbors push back with equal force — it is pressure *differences* that result in acceleration. This suggests that force per volume at a point is the limit of a difference quotient,[2] the negative gradient $-\boldsymbol{\nabla} p$ of the pressure. (The gradient operator $\boldsymbol{\nabla}$ is introduced in equation (15) of Appendix A.1. Here, it is understood to

[1] The mass contained in each finite sub-volume V is then given by the integral of ρ over the sub-volume.

[2] Consider a small box-shaped sub-volume of fluid, say of lengths (a, b, c) in the three coordinate directions. Denote the three components of force acting on the box by F_1, F_2, and F_3. Then F_1, the x_1-component of force acting on the entire box, equals the difference of pressures at the left and right ends of the box, multiplied by bc, the area of the right and left faces. To first order, this pressure difference is $-a\,\partial p/\partial x_1$, so $F_1 \approx -abc\,\partial p/\partial x_1$, and similarly for the other coordinate directions, so that $\boldsymbol{F} \approx -abc\,\boldsymbol{\nabla} p$. In the limit $a, b, c \to 0$, the higher order corrections tend to zero at a faster rate and $-\boldsymbol{\nabla} p$ remains as an exact expression for the force per volume.

act only on the space variables $\boldsymbol{x}$.) We note that the force is directed toward areas of low pressure, hence the minus sign. Equating our two expressions for force per volume, we conclude that Newton's law for a fluid reads

$$-\boldsymbol{\nabla} p(\boldsymbol{x}(t),t) = \rho(\boldsymbol{x}(t),t)\,\frac{\mathrm{d}^2\boldsymbol{x}(t)}{\mathrm{d}t^2}\,. \tag{1}$$

In principle, this is the equation we want. However, it is not quite useful yet because it mixes so-called *Eulerian quantities* and *Lagrangian quantities*. Eulerian quantities are properties of the fluid which are functions of the current position $\boldsymbol{x}$, while Lagrangian quantities are functions of the initial location, or "particle label" $\boldsymbol{\xi}$. So pressure and density are Eulerian[3] while the particle position $\boldsymbol{x}$ itself, the velocity $\mathrm{d}\boldsymbol{x}/\mathrm{d}t$, and the acceleration $\mathrm{d}^2\boldsymbol{x}/\mathrm{d}t^2$ are Lagrangian. For most purposes it is much more convenient to re-express (1) in terms of all-Eulerian quantities: writing $\boldsymbol{u}(\boldsymbol{x},t)$ to denote the velocity felt by a *stationary* observer at location $\boldsymbol{x}$ and time t, we observe that

$$\frac{\mathrm{d}\boldsymbol{x}(t)}{\mathrm{d}t} = \boldsymbol{u}(\boldsymbol{x}(t),t)\,. \tag{2}$$

Differentiating in time and using the chain rule of multivariable calculus (17) explained in Appendix A.1, we obtain a fully Eulerian expression for the acceleration of the particle,

$$\frac{\mathrm{d}^2\boldsymbol{x}(t)}{\mathrm{d}t^2} = \frac{\partial \boldsymbol{u}}{\partial t}(\boldsymbol{x}(t),t) + \boldsymbol{u}(\boldsymbol{x}(t),t)\cdot\boldsymbol{\nabla}\boldsymbol{u}(\boldsymbol{x}(t),t)\,. \tag{3}$$

Inserting (3) into (1) and dropping all arguments for simplicity, we arrive at a form of Newton's law which was first introduced by Euler in 1757:

$$\rho\left(\frac{\partial \boldsymbol{u}}{\partial t} + \boldsymbol{u}\cdot\boldsymbol{\nabla}\boldsymbol{u}\right) + \boldsymbol{\nabla} p = 0\,. \tag{4}$$

A fluid governed by (4) is called *ideal*: the model neglects possible frictional forces which can turn kinetic energy into heat and other effects caused by the molecular structure of a real fluid.

At this point, we have more unknown functions than we have equations (the d components of $\boldsymbol{u}$, pressure p, and density ρ are unknowns, but (4) provides only d equations). So we need more information coming from physics. The question is essentially this: what happens to the density when the pressure changes? There is no general answer as a gas will behave differently than, e.g., water. In this contribution, we focus on the case where the fluid is incompressible: the volume of arbitrary parcels pushed around by the flow

[3] In (1), the Eulerian quantities $\boldsymbol{\nabla} p$ and ρ are evaluated at the current position $\boldsymbol{x}(t)$ of a Lagrangian particle, so they are read as Lagrangian quantities. The gradient, however, must be computed with respect to Eulerian position coordinates $\boldsymbol{x}$ rather than Lagrangian labels $\boldsymbol{\xi}$.

(such as V_t in Figure 1) does not change over time.[4] The relative rate of change of a parcel volume, in the limit of vanishing size, is measured by a quantity called the divergence of the velocity field $\boldsymbol{u}$, see Appendix A.2. In particular, the flow of $\boldsymbol{u}$ is incompressible if and only if $\operatorname{div} \boldsymbol{u} = 0$.

For simplicity, we also assume that the fluid is *homogeneous*: fluid parcels not only maintain their volume as they are pushed around by the flow, but have constant density throughout the fluid domain.[5] Then, with appropriate normalization, we can take $\rho \equiv 1$. What results are the *Euler equations* for a homogeneous incompressible ideal fluid,

$$\frac{\partial \boldsymbol{u}}{\partial t} + \boldsymbol{u} \cdot \boldsymbol{\nabla} \boldsymbol{u} + \boldsymbol{\nabla} p = 0\,, \tag{5a}$$

$$\operatorname{div} \boldsymbol{u} = 0\,. \tag{5b}$$

The pressure in incompressible flow is determined solely by the condition that each sub-volume must move consistently with the motion of all of its neighbors. The resulting pressure force generates the necessary instantaneous adjustment across the entire fluid domain.

So far, we have neglected friction. Due to its fundamental theoretical and practical implications, we shall look at friction in more detail. Frictional forces enhance the local coherence of the flow, i.e. they counteract, at each point, the deviation of the velocity field from its local average: if a particle moves faster than the average of its neighbors, then friction slows it down. The deviation of a function at a point from its average value on small surrounding spheres is measured by the negative of the *Laplacian* Δ, a differential operator explained in Appendix A.3, so that frictional forces should be proportional to $\Delta \boldsymbol{u}$. Adding such a term to the Euler equations (5), we obtain the *Navier–Stokes equations* for a homogeneous incompressible fluid,

$$\frac{\partial \boldsymbol{u}}{\partial t} + \boldsymbol{u} \cdot \boldsymbol{\nabla} \boldsymbol{u} + \boldsymbol{\nabla} p = \nu\, \Delta \boldsymbol{u}\,, \tag{6a}$$

$$\operatorname{div} \boldsymbol{u} = 0\,. \tag{6b}$$

[4] There are certain physical effects that can only be described by a compressible model, such as acoustic waves, shock formation, and supersonic flows. If these are important, the model must be augmented with the appropriate laws of thermodynamics; in this more general case, the pressure forces are due to local imbalances in the internal energy or temperature. However, the usual state of the flow of water and the macroscopic motion of air are well described as being incompressible. There is also a computational motivation for considering incompressible flows: the effects of compressibility usually take place on much smaller scales than the motion of the bulk. These are expensive to resolve properly. Moreover, in situations where compressible effects are physically negligible, simulations of the compressible model which do not properly resolve such small scales may be very "unstable" so that it is better to start with an incompressible model right away.

[5] This is a rather mild restriction as the case of non-constant density incompressible flow is mathematically very similar to the special case considered here.

The constant $\nu > 0$ is called *coefficient of viscosity* and describes the strength of the viscous forces; it is much larger for honey, for example, than it is for water. Note that the same right hand term, $\nu\Delta\boldsymbol{u}$, appears for the same reason when modeling the flow of heat or the diffusion of a chemical; one such example is described by L.N. Trefethen in this volume [18].

The partial differential equations (5) and (6) are examples of *initial-boundary value problems*: this means that, in order to determine the flow completely, we need to specify both *initial* and *boundary values* to compute the velocity field for later times $t > 0$. For the purpose of this discussion, we assume *periodic boundary conditions* on a box-shaped domain Ω: we can think of tiling the whole of $\mathbb{R}^d$ with an array of exact copies of our domain Ω, thereby matching corresponding points at opposite faces of the box. Thus, what flows out one face of Ω appears to come back in at the opposite face.

For more physically realistic boundaries, one might alternatively specify the fluxes across the boundary — the amount of fluid moving in or out of the domain. For a Navier–Stokes flow, momentum fluxes due to the frictional forces on the boundaries are also required; this holds true even in situations where the energy dissipation due to friction is negligible — a crucial difference which is necessary for explaining lift on an aircraft wing. Here, however, we shall not consider boundary issues further; we take the point of view that fluid dynamics with periodic boundary condition is prototypical for fluid flow far away from real boundaries.

3 Conservation Laws

In classical mechanics, there are three fundamental conserved quantities: momentum, energy, and angular momentum. Each has a fluid analogue which provides important structural information. Conservation of momentum is the essence of Newton's second law and therefore already part of the picture. The kinetic energy of a point-particle is given by the expression $E = \frac{1}{2}m|\boldsymbol{v}|^2$. In a continuum, as we replace mass m by the mass density ρ, we correspondingly replace E by the kinetic energy density $\frac{1}{2}\rho|\boldsymbol{u}|^2$. For incompressible flow, all energy is kinetic, so that the total energy is obtained by integrating the kinetic energy density over the fluid domain. Here, with $\rho = 1$, the total energy reads

$$E = \frac{1}{2}\int_\Omega |\boldsymbol{u}|^2 \,\mathrm{d}\boldsymbol{x}\,. \tag{7}$$

A simple computation, detailed in Appendix B.1, shows that E remains constant under the flow of the Euler equations and is decreasing for Navier–Stokes flow where friction turns kinetic energy into heat.

What remains are conservation laws related to rotation. For Newton's equations of particle mechanics, the conserved quantity is called *angular momentum*, always defined relative to a reference point. In fluid mechanics,

matters are more complicated. Instead of a reference point we must consider closed curves C_t which are transported by the flow, i.e. $C_t = \mathbf{\Phi}_t(C_0)$. Relative to any such curve, the *circulation* is defined by the line integral

$$\Gamma_t = \oint_{C_t} \boldsymbol{u} \cdot \mathrm{d}\boldsymbol{s} \tag{8}$$

which is computed by summing up the components of the velocity field which are tangent to C_t, see Appendix A.4. Each such Γ_t is a constant of motion for the Euler equations. Moreover, due to Stokes' theorem as explained in Appendix A.4, the circulation equals the surface integral

$$\Gamma_t = \int_{S_t} \boldsymbol{\omega} \cdot \mathrm{d}\boldsymbol{A}\,, \tag{9}$$

where S_t is any oriented surface, again moving with the flow, whose boundary is the curve C_t, and where $\boldsymbol{\omega}$ denotes the *vorticity*

$$\boldsymbol{\omega} = \operatorname{curl} \boldsymbol{u} = \Big(\frac{\partial u_3}{\partial x_2} - \frac{\partial u_2}{\partial x_3}, \frac{\partial u_1}{\partial x_3} - \frac{\partial u_3}{\partial x_1}, \frac{\partial u_2}{\partial x_1} - \frac{\partial u_1}{\partial x_2}\Big)\,. \tag{10}$$

The i-th component of the vorticity vector can be seen as the limit circulation per unit area in the plane perpendicular to the x_i-direction. Intuitively, it measures how much a little leaf carried by the flow would spin about the i-th coordinate vector. In two space dimensions, only the third component of (10) is nonzero and vorticity can be identified with the scalar $\partial u_2/\partial x_1 - \partial u_1/\partial x_2$.

Circulation highlights a crucial difference between flows in two and in three dimensions: since "volume" in two dimensions coincides with the notion of area, incompressibility implies that the area of S_t is a constant of the motion. In the limit of arbitrarily small area of S_0, equation (9) shows that conservation of circulation implies conservation of vorticity along flow lines. In three dimensions, there is no constraint on the area of S_t under volume-preserving transformations. Hence, conservation of circulation cannot control the magnitude of the vorticity vector. This is the reason for the qualitative differences between flow in two and three dimensions, and why the two-dimensional equations cannot have singularities, but the three-dimensional equations might.

The importance of vorticity and circulation for the question of singularity formation can be understood by a simple thought experiment. Start with a balloon filled with an incompressible non-viscous fluid at rest and tie a lasso around its waist which is contracted to a point in a finite time, forcing the fluid into two lobes above and below its waist as in Figure 2. Clearly, we have created a topological singularity as we close off the two lobes from each other at a point. Velocity and vorticity of the fluid, however, remain bounded.

Now repeat the thought experiment with a fluid inside the balloon rotating about its axis. In this example, the velocity is always tangent to the lasso so that (per the definition of the line integral) the circulation is obtained by

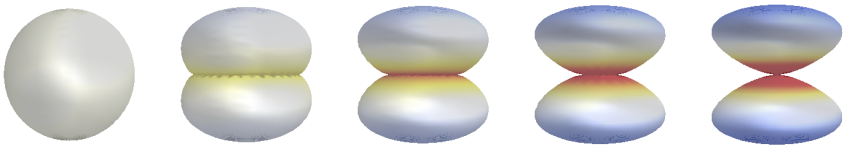

Fig. 2. Illustration of the rotating balloon thought experiment. As the lasso contracts, conservation of circulation implies that the velocity along the waist increases (indicated by red colors) while the velocity on the outer lobes decreases (indicated by blue colors).

integrating the magnitude of the velocity along a circle on the surface of the balloon, which is given by the product of fluid speed and the circumference of the opening. Conservation of circulation demands that both fluid speed and vorticity become infinite near the lasso as it closes, see Figure 2. This is much like an ice-skater who turns faster and faster as she moves all her mass towards the axis of her pirouette, propelled just by conservation of angular momentum. This scenario creates a much stronger singularity than the first.

The blowup question for fluids asks if any of these (or possibly other) scenarios of singularity formation may be the result of the action of a flow onto itself. For the Euler equations, it is known that any singularity is necessarily a singularity in the vorticity; this is discussed with more detail in Section 7. So the squeezing off of the rotating balloon could possibly be the movement of a sub-volume in a singular flow, while the squeezing off of the nonrotating balloon can never occur as the most singular event in the interior of a flow. For the Navier–Stokes equations, friction would prevent the velocity from becoming singular in these simple thought experiments, but in general, the question remains open, as we explain next.

4 The Clay Millennium Problem

For a mathematician, the first question when studying partial differential equations like (5) or (6) is their *well-posedness*: (i) existence of solutions — the physical system must have a way to evolve into the future, (ii) uniqueness — there must not be arbitrary choices for the evolution, and (iii) continuous dependence on the initial state — any future state is determined, to arbitrary finite precision, by the initial conditions to a sufficient finite precision.

For the incompressible Euler and Navier–Stokes equations, a complete answer to these questions is open. What is known is that both are *locally well-posed*: solutions starting out from smooth (infinitely differentiable) initial data are unique, depend continuously on the initial data, and remain smooth for at least a finite, possibly short, interval of time. Proofs of local well-

posedness can be achieved by formulating the equations as a fixed point problem in a suitable space X of functions. Doing so discards much of the problem-specific structure, but we can hope to continue the solution for all times by noting that this local existence argument permits only one of the following alternatives: either the solution exists on the entire interval $[0, \infty)$ of times, or the solution exists only on some finite interval $[0, T^*)$ of times and the size of the solution, called the "norm in X", diverges as $t \to T^*$. In the latter instance, we say colloquially that the solution is "blowing up at time T^*". Hence, proving global well-posedness reduces to finding a bound on the norm in X for every $t > 0$.

The question of whether arbitrary smooth solutions of the incompressible Navier–Stokes equations in three space dimensions can be continued globally in time in this manner is now one of the seven Millennium Prize Problems posed by the Clay Mathematics Institute. It is stated as follows [8]. Either *prove that initially smooth solutions with periodic boundary conditions (or in* $\mathbb{R}^3$ *with strong decay conditions toward infinity) remain smooth for all times*, or *find at least one solution which blows up in finite time.* Global well-posedness for the three-dimensional incompressible Euler equations remains equally open, but is not covered by the Clay prize question.

Let us sketch some partial results. For the Euler equations in two space dimensions, we have already argued that vorticity is conserved as a scalar along flow lines. This is sufficient to prevent blowup of finite energy solutions. For Navier–Stokes in two dimensions, the dissipation of energy due to friction is sufficiently strong so that the same conclusion can also be derived via "energy estimates" which are described in more detail in Appendix B.

Even in three dimensions, solutions to the Navier–Stokes equations with general initial data can be continued past the time of their first possible singularities as "weak" or "generalized" solutions.[6] Weak solutions exist globally in time; however, it is physically troublesome that they are not known to be unique. For the three-dimensional Euler equations, only special classes of weak solutions are known; there are also examples of non-uniqueness.

It is further known that "small" solutions of the Navier–Stokes equations do not blow up. Much effort has been spent on characterizing smallness, e.g. in terms of the smallness of the initial data, of the viscosity being large, or of the solution being in some sense close to some known special solution or symmetry. Physically, all such cases can be characterized as being non-turbulent: diffusion $\nu\Delta\boldsymbol{u}$ is, in some specific sense, so strong that any perturbation coming from the $\boldsymbol{u} \cdot \boldsymbol{\nabla u}$ term is damped away before it could lead to singularities. Intuitively, if a fluid equation for water is in danger of developing singularities, we replace the water by honey, and if the honey is sufficiently viscous, no singularities can develop. Obviously, such results are not avail-

[6] Although such a solution may be discontinuous or even singular, averages of the solution over small finite sub-volumes can still depend continuously on the initial state. Interpreted this way, condition (iii) in the notion of well-posedness may still be satisfied.

able for the Euler equations where $\nu = 0$. Another class of results known to hold for Navier–Stokes, but not for Euler, are so-called partial regularity results which, based on more subtle measure-theoretic arguments, state that the space-time set of singular points of weak solutions is in a certain sense small.

As a further surprise, there are known blowup solutions to both Euler and Navier–Stokes equations on unbounded domains in three as well as two dimensions. However, even before blowup, their kinetic energy per volume is also unbounded. Unbounded local energy implies, in particular, that arbitrarily large velocities arise, which cannot happen in a real physical system. Such solutions are also not covered by the Clay prize question.

5 To Blow Up or Not To Blow Up?

Let us consider a few inconclusive arguments which shape our beliefs in whether or not solutions to the Euler or Navier–Stokes equations blow up. An often cited but potentially misleading analogy are Burgers' equations, taken either with or without viscosity. These equations are obtained, respectively, from the Navier–Stokes and Euler equations by setting $p = 0$ and dropping the incompressibility constraint. These equations are not a physical model, but are of theoretical interest as a clear black-and-white picture emerges: without viscosity, each particle keeps its initial velocity and blowup occurs in the form of particle collisions. With viscosity, the global maximum of velocity remains nonincreasing and friction is strong enough to prevent blowup [12].

There is no reason to expect that the same pattern, namely, that blowup occurs if and only if viscosity is absent, pertains to real fluids. The two systems are different in very fundamental ways: for real fluid flow, there is no mechanism which can give us direct control on the magnitude of the velocity field; the difficulty arises from the coupling between transport, an inherently local phenomenon, with pressure forces which are due to the global interaction of all fluid particles. So one might think that Euler and Navier–Stokes behave worse than Burgers' equations. However, there is clear evidence that pressure stabilizes incompressible flow to some extent. In two dimensions, as we recall, we can now control the magnitude of vorticity which implies the existence of global regular solutions with or without viscosity. In three dimensions, as this control is lost, all bets are off.

Despite this, many believe that either, or both, Euler or Navier–Stokes flows develop singularities. Why? One reason is related to the *cumulative energy dissipation*

$$\nu \int_0^t \int_\Omega |\boldsymbol{\nabla} \boldsymbol{u}|^2 \, \mathrm{d}\boldsymbol{x} \, \mathrm{d}t \,. \tag{11}$$

This quantity measures how much energy has been lost up to time t, as is explicitly shown in Appendix B.1. We would expect that, over a fixed

interval of time $[0, t]$, this quantity is continuous as a function of ν. However, there is strong numerical and experimental evidence that the cumulative energy dissipation does not converge to zero as $\nu \to 0$. This phenomenon is referred to as *anomalous dissipation* and is assumed in most attempts to model turbulence [7]. Mathematically, anomalous dissipation implies loss of smoothness at least for the Euler equations. Its implications for the Navier–Stokes equations are less clear.

Suppose, for the sake of argument, that Euler solutions do blow up, but Navier–Stokes solutions don't. Then regularity for the Navier–Stokes equations should come from the viscous term. However, the known mechanisms in which viscosity acts do not suffice to prove that viscosity could always control the nonlinearity. (For example, in L.N. Trefethen's model blowup problem [18], the diffusive term is insufficiently strong to prevent blowup.) So unless there is a yet unknown magical mechanism, at least some Navier–Stokes solutions might blow up, too.

So why do others believe that the Euler and Navier–Stokes equations do not have singularities? There are two reasons. First, because the numerical evidence remains, despite much effort, inconclusive. There are simulations on both sides of the argument [3, 11, 13, 15] none of which, however, establishes a "road to blowup" as is known for other models. Second, because once the continuum description of fluids is accepted, there is nothing obviously missing or incomplete. This is bolstered by the success of the Navier–Stokes equations as a deterministic theory when compared with almost every piece of experimental evidence.

6 Collapse of Vortex Tubes

Let us now look more closely at the role that simulation might play in solving the blowup problem. As with experiments in a real-world laboratory, before embarking on any sort of computational experimentation, one must first identify computational scenarios which would provide the most insight within the hardware and algorithmic constraints under which we must operate.

Our objective is to find configurations which quickly develop localized intense dynamics. Such scenarios can then be probed for signs of singularity formation or for signs of depletion of the nonlinear self-amplification. Initialization with random data was used first and indicated that intense events tend to occur in tube-like structure that rotate about their axis of symmetry. They are referred to as *vortex tubes* and occur in many natural flows, including tornadoes descending from strongly rotating storms or around the rising parcels of heated air in afternoon thunder clouds. Vortex tubes are often not easily visible, but can be visualized through condensation due to the low pressure in the vortex cores, air bubbles sucked into the cores, or injection of dye.

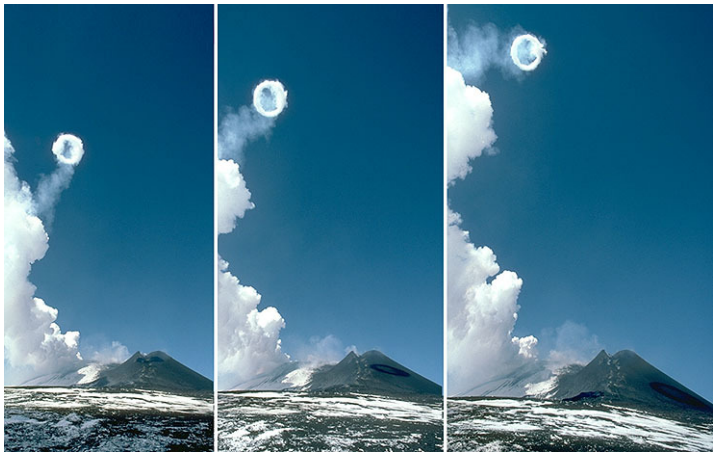

Fig. 3. Self-propagating steam rings ejected from an eruption at the south east crater of the volcano Etna in 2000. Notice how the shadow of the ring travels across the slope. Photos by Juerg Alean from `http://www.swisseduc.ch/stromboli/etna/etna00/etna0002photovideo-en.html?id=4`.

Simulations and data from experiments indicate two further trends. Vortices in turbulent flows amplify by stretching, much as in the rotating balloon thought experiment in Section 3. And the most intense events, if not the most frequent, tend to involve pairs of parallel counter-rotating ("antiparallel") vortex tubes which initially self-propagate. This is why many studies of singularity formation focus on such pairs [15]. There are also high resolution studies with smooth, highly symmetric initial conditions which might be showing signs of similar singular behavior [11]. Simulations with random data continue to play a crucial role in the study of turbulence, but are now considered too "noisy" to reveal the local structure of possible singularity formation.

In a flow without viscosity, two exactly linear, antiparallel vortex tubes will simply propagate at constant velocity. Similarly, vortex rings, which can appear as smoke rings, are a beautiful example of self-propagation: diagonally across the core, the direction of vorticity is anti-aligned, pushing fluid through the center and dragging the vortex ring with it; see Figure 3. Another good example of self-propagation and subsequent break-down are the vortices shed by aircraft wings. Sometimes they are visible as condensation trails, where water vapor condenses due to pressure and temperature drops in the vortex cores; they can also be made visible by smoke generators, as in the NASA study shown in Figure 4. (Typical high-altitude aircraft condensation trails come from the outflow of jet engines, but eventually they are engulfed by the wing-tip vortices.) Further downstream, these tube-like structures are twisting and starting to attract one another. This is known as the Crow in-

Fig. 4. This picture shows the wing-tip vortices which are associated with the circulation generating lift coming off the wings of a Boeing 727 aircraft. They were made visible by smoke generators installed on the tips of the aircraft wings. (NASA photograph number ECN-3831.)

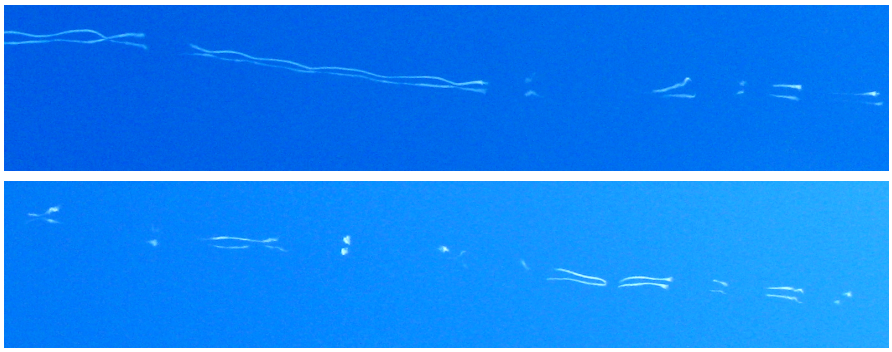

Fig. 5. Breakdown via the so-called Crow instability of a pair of vortex tubes trailing an aircraft. What is seen is the interaction of the vortices with the condensation trail from the jet engines; the lower half of the picture continues the upper half on the right. From `http://commons.wikimedia.org/wiki/File:The_Crow_Instability.jpg`.

stability; see Figure 5. Eventually, the tubes will touch and reconnect, before becoming turbulent and disappearing.

Why are the two vortex tubes attracted to one another? When an exactly linear self-propagating pair of vortex tubes is perturbed, the tubes will be stretched somewhere along their axis. Under incompressibility, this must be compensated for by compression in the perpendicular directions. The tubes become longer and thinner, much as when chewing gum is pulled, and move closer together; see Figure 6. This mechanism is self-amplifying and leads to a rapid generation of small scale structures, as in Figure 7. Many measures of the complexity of the flow, especially vorticity and pressure gradients, grow

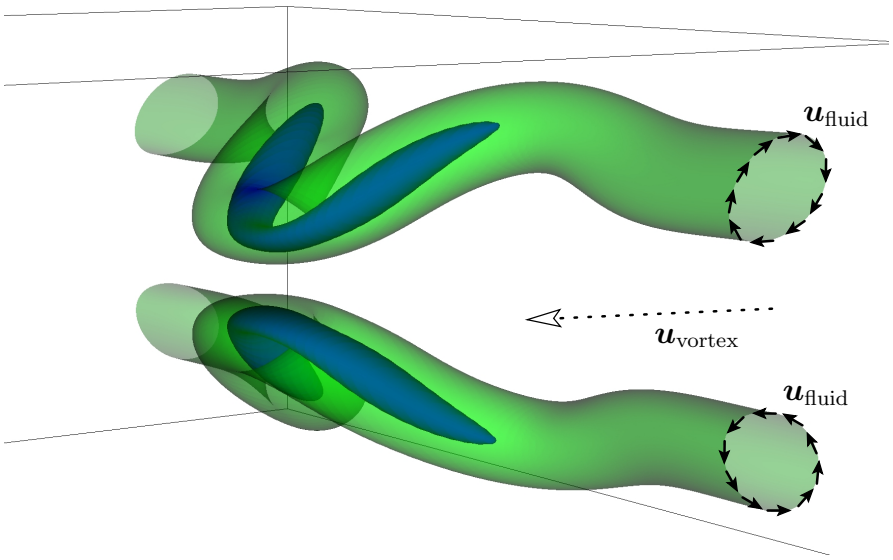

Fig. 6. Two antiparallel vortex tubes. The true velocity of the flow is marked $\boldsymbol{u}_{\text{fluid}}$; the apparent direction of propagation of the vortex structure is indicated as $\boldsymbol{u}_{\text{vortex}}$. The colored surfaces are surfaces of constant vorticity modulus at 60% and 90% of peak vorticity. From [3].

around these structures. One of the questions that remain unanswered is this: do pressure gradients contribute to the amplification of vorticity, or do they suppress any possible blowup by repelling the vortices and flattening them? Both trends have been observed, depending upon the initial conditions or, adding to the mystery, upon what stage of the evolution is considered.

7 Numerical Error

In areas such as number theory or discrete mathematics, computers can find examples or counterexamples; sometimes it is even possible to achieve computer-assisted proofs. The space-time continuum of fluid motion, however, can only be approximated on a discrete computational mesh by finitely many floating point values. Consequently, computers are fundamentally incapable of *proving* that solutions to the Euler or Navier–Stokes problems are well-behaved. On the other hand, *knowing* that the solutions are well-behaved, we can prove that, given sufficient computational resources, we could numerically solve the equation to any required accuracy. Yet, there are many ways how computations interact with mathematical analysis to provide us with a better understanding of the blowup question. Given the

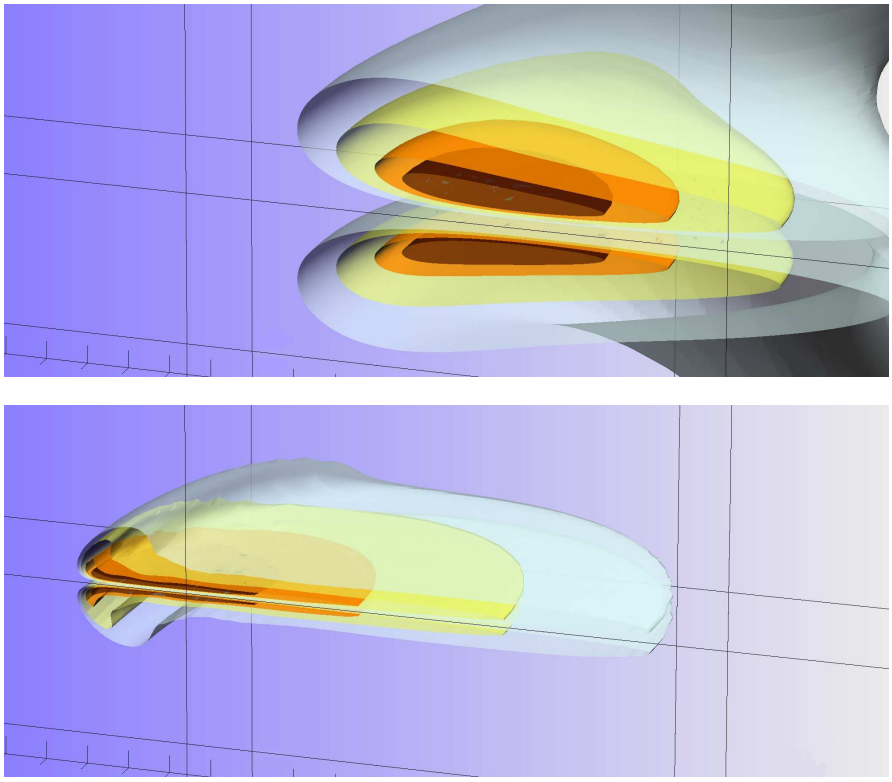

Fig. 7. Collapse of two antiparallel vortex tubes. Snapshots at $t = 5.6$ and $t = 8.1$ with a conjectured time of singularity $T^* \approx 11$. From [3].

proper configurations, simulations can inspire conjectures, validate assumptions, and probe the properties of inequalities.

A large number of numerical approximation methods ("schemes") for fluid equations have been devised, each with distinct advantages and disadvantages. For example, many engineering problems use adaptive schemes that refine the computational mesh locally in regions of interest. Sometimes it is also possible to choose an initial condition which makes optimal use of a fixed computational mesh, and then use simple and fast numerics, such as spectral methods as detailed in Appendix C.

No matter which approach is used, a near-singular flow will develop small scale features which cannot be represented well with a fixed and finite number of degrees of freedom. As the flow develops, errors will grow, so that we need some means of validating the accuracy of the computation. The most complete validation possible would be to refine on progressively finer meshes, requiring progressively larger computers. Since this is impossible from a practical point of view, the usual compromise is to monitor the preservation of

invariants and check for anomalous growth of small scale features for a few refined mesh calculations. When carefully done, this can provide us with a reasonable degree of confidence in the quality of the simulation.

Validation of numerical results becomes easier when the equations possess symmetries and conservation laws. For this reason, almost all blowup studies are done on the Euler rather than the Navier–Stokes equations. An additional benefit of looking at non-viscous flow is that one can study the geometry of vortex stretching without possible interference of viscous effects.

Besides validation, we need computable measures to decide whether a particular simulation result might be singular, or is clearly nonsingular. The most famous such criterion is the Beale–Kato–Majda bound for the Euler equations [1], which says that

$$\int_0^{T^*} \max_{\boldsymbol{x}\in\Omega} |\boldsymbol{\omega}(\boldsymbol{x},t)|\,\mathrm{d}t = \infty \tag{12}$$

is necessary and sufficient for blowup at time T^*. This criterion is important for two reasons. First, it gives a bound on how fast singularities can develop: the peak vorticity must blow up essentially at least as fast as $(T^*-t)^{-1}$. Second, there can be no singularities in higher derivatives of velocity in the Euler equations unless there is a singularity in the vorticity, which is a first derivative of the velocity and usually easily calculable.

The publication of this calculable test in 1984 fueled a decade of numerical activity aimed at identifying either singular structures, or mechanisms for suppressing singular trends. However, no scientific consensus had been reached, with only one calculation [14] providing modest consistency with a power law singularity while maintaining sufficient resolution in all three directions. It also became apparent that the Beale–Kato–Majda criterion by itself was insufficient for discriminating between the competing claims. Several additional tests for singular behavior that are both independent and calculable were subsequently proposed [2, 5, 13, 16]. Still, whether the strongest claims for singular behavior are consistent with the mathematical bounds remains an open question [3, 13]. It now appears feasible that a consolidated effort involving adequate high performance computing resources, the latest in adaptive mesh methods, and the use of better initial perturbation profiles could either substantiate the proposed singular scaling regime, or would clearly show how the nonlinearities generate a negative feedback that suppresses singular trends.

8 An Invitation to Research

New blowup criteria — some that are more robust, as well as some that are more refined — could make a real difference. Numerically robust tests would involve space integrals or averages. One candidate might be the enstrophy,

the integral over the square of the vorticity, which appears promising but needs theoretical support. In [3], for example, the Euler enstrophy appears to follow a power law consistent with the best known upper bound on the growth of enstrophy in the Navier–Stokes equations. Whether this is coincidental or whether there is a deeper connection remains a mystery. More refined blowup tests, on the other hand, might make explicit reference to the local geometry of vortex lines and vortex structures.

More generally, there remain open questions about the relationship between the Navier–Stokes and Euler equations. In the presence of boundaries, the limit of vanishing viscosity is still not well understood [2]. Further, it remains a mystery whether a global regularity result for Euler would imply one for Navier–Stokes, as one would naively expect because one would think viscosity can only dampen the development of singularities [5]. Nonetheless, we believe that a breakthrough on the Navier–Stokes problem will come via a breakthrough on the Euler problem. One reason is that the Navier–Stokes viscosity is mathematically well understood, yet is insufficient to control the nonlinearity. Another reason is that the Euler equations have conservation laws, while the Navier–Stokes equations do not, which can be used to monitor the reliability of numerical simulations probing for blowup.

Independent of these hard problems, it is always worthwhile building intuition with lower dimensional toy problems which share some similarity with the three-dimensional Navier–Stokes and Euler equations. In some cases, simulations have been used to predict existence and non-existence of singularities. The extreme situations created to address these issues, often found after a painful period of numerical experimentation, continue to inspire new mathematics which is then used to validate numerical predictions.

In practical applications, one can often "model" the effects of small scales which cannot be resolved computationally. In "large eddy simulations", for example, the Navier–Stokes viscous term is replaced by an eddy viscosity designed to represent the average effects of viscosity over a computational cell. In a global weather calculation, almost everything is modeled. Such approaches are often successful in preserving crucial statistical properties of the solution; their importance cannot be overestimated, yet their mathematical study remains wide open. Especially needed is the development of new mathematical concepts to address the relation of accuracy at large scales to a probabilistic notion of accuracy at small scales.

Mathematical fluid dynamics and, more generally, partial differential equations is a field where analysis, physics, and computation meet and frequently progress jointly. It is a field where deep mathematical questions and application driven problems sit side by side. And it is a field which, at this point in its long history, is as vibrant as ever.

Appendix A. A Brief Guided Tour of Vector Calculus

For functions in one variable, the derivative $f' = \mathrm{d}f/\mathrm{d}x$ denotes the local rate of change of f per unit distance, and the fundamental theorem of calculus relates these local rates to the global change of f within an interval $[a, b]$. For functions in several variables, as necessarily occur when modeling fluid flow, local rates of change are measured by directional derivatives which give rise to four important differential operators: gradient, divergence, curl, and Laplacian. These differential operators describe local properties of a function or vector field which are related to global changes via the integral theorems of Gauss and Stokes. We will explain these basic concepts without proofs and precise statements of assumptions under the premise that our readers are already familiar with single variable calculus and some analytic geometry. For further background, there are many excellent textbooks and we encourage the reader to find his or her favorite, or to search on the internet.

A.1 Directional Derivative, Gradient, and Chain Rule

Let $U \subset \mathbb{R}^n$ be an open set, $f\colon U \to \mathbb{R}$ a function, and consider a point $\boldsymbol{x} = (x_1, \dots, x_n) \in U$. (We use boldface symbols for vector-valued variables or functions, and plain symbols for real-valued variables or functions.) We ask for the rate of change of f as we vary its argument $\boldsymbol{x}$ in some direction $\boldsymbol{v} = (v_1, \dots, v_n) \in \mathbb{R}^n$. This question can be answered by taking the single-variable derivative of the function $t \mapsto f(\boldsymbol{x} + t\boldsymbol{v})$, which is well-defined for small values of t. Then the local rate of change,

$$\left.\frac{\mathrm{d}f(\boldsymbol{x} + t\boldsymbol{v})}{\mathrm{d}t}\right|_{t=0} = \lim_{t\to 0} \frac{f(\boldsymbol{x} + t\boldsymbol{v}) - f(\boldsymbol{x})}{t}\,, \tag{13}$$

if it exists, is called the *directional derivative* of f at $\boldsymbol{x}$ in the direction $\boldsymbol{v}$.[7]

When $\boldsymbol{v} = (0, \dots, 0, 1, 0, \dots, 0)$ is a unit vector with a single 1 in the i-th coordinate, the associated directional derivative is referred to as the i-th *partial derivative*, written $\partial f/\partial x_i$ or $\partial_i f$ for short. It is computed by taking the single-variable derivative of f with respect to x_i while holding the remaining components of $\boldsymbol{x}$ constant.

More generally, we can look at the rate of change of f as its argument changes along an arbitrary smooth curve which is parameterized by a function $\boldsymbol{\phi}\colon (a, b) \to U$. The vector components of $\boldsymbol{\phi}$ are denoted $\phi_1, \dots, \phi_n$, so that $\boldsymbol{\phi}(t) = (\phi_1(t), \dots, \phi_n(t))$. Then the multivariate *chain rule* asserts that

$$\frac{\mathrm{d}}{\mathrm{d}t} f(\boldsymbol{\phi}(t)) = \sum_{i=1}^{n} \frac{\mathrm{d}\phi_i(t)}{\mathrm{d}t} \left.\frac{\partial f}{\partial x_i}\right|_{\boldsymbol{x}=\boldsymbol{\phi}(t)}. \tag{14}$$

[7] The "vertical bar" notation used in (13) and subsequent expressions indicates that the derivative should be computed *before* the indicated argument substitution is applied.

The sum in this expression can be understood as a vector dot product between $\mathrm{d}\boldsymbol{\phi}/\mathrm{d}t = (\mathrm{d}\phi_1/\mathrm{d}t, \ldots, \mathrm{d}\phi_n/\mathrm{d}t)$, which can be thought of as the velocity of a point moving on the curve, and the vector of partial derivatives

$$\boldsymbol{\nabla} f \equiv (\partial f/\partial x_1, \ldots, \partial f/\partial x_n)\,, \tag{15}$$

which is called the *gradient* of f. Using familiar dot product notation $\boldsymbol{u}\cdot\boldsymbol{v} = u_1\,v_1 + \cdots + u_n\,v_n$, we can then write the chain rule (14) as

$$\frac{\mathrm{d}}{\mathrm{d}t} f(\boldsymbol{\phi}(t)) = \frac{\mathrm{d}\boldsymbol{\phi}(t)}{\mathrm{d}t} \cdot \boldsymbol{\nabla} f\big|_{\boldsymbol{x}=\boldsymbol{\phi}(t)}\,. \tag{16}$$

This is like the one-dimensional chain rule $(f(\phi(t))' = \phi'(t)\,f'(\phi(t))$, except we have to take the contributions in all n coordinate directions into account.

Applying the chain rule with $\boldsymbol{\phi}(t) = \boldsymbol{x} + t\boldsymbol{v}$ so that $\mathrm{d}\boldsymbol{\phi}/\mathrm{d}t = \boldsymbol{v}$, we find that $\boldsymbol{v}\cdot\boldsymbol{\nabla} f$ expresses the directional derivative of f in the direction $\boldsymbol{v}$. Among all vectors $\boldsymbol{v}$ of unit length, $\boldsymbol{v}\cdot\boldsymbol{\nabla} f$ is maximal when $\boldsymbol{v}$ aligns with $\boldsymbol{\nabla} f$; we conclude that the gradient $\boldsymbol{\nabla} f$ is a vector which points into the direction in which f has the greatest directional derivative at $\boldsymbol{x}$, and that the magnitude of $\boldsymbol{\nabla} f$ is the directional derivative of f in this direction. It is often convenient to think of $\boldsymbol{\nabla} = (\partial_1, \ldots, \partial_n)$ as a vector of differentiation symbols.

A *vector field* is a function $\boldsymbol{u}\colon U \to \mathbb{R}^n$ which assigns a vector to each $\boldsymbol{x} \in U$. A typical example is a fluid which has, at each point, a velocity vector $\boldsymbol{u}(\boldsymbol{x})$. When applying the directional derivative $\boldsymbol{u}\cdot\boldsymbol{\nabla}$ to a vector field $\boldsymbol{v}$, it acts on each component separately, i.e., $\boldsymbol{u}\cdot\boldsymbol{\nabla}\boldsymbol{v} = (\boldsymbol{u}\cdot\boldsymbol{\nabla} v_1, \ldots, \boldsymbol{u}\cdot\boldsymbol{\nabla} v_n)$.

In fluid dynamics, we typically encounter time dependent functions and vector fields. Hence, we must notationally distinguish the space variables $\boldsymbol{x}$ from time t. We write $\boldsymbol{x} \in \Omega \subset \mathbb{R}^d$ (usually with $d = 2$ or $d = 3$) to denote a point in our fluid domain, and (a, b) for a time interval. We use $\boldsymbol{\nabla} = (\partial_1, \ldots, \partial_d)$ to denote the gradient with respect to the space coordinates only, and ∂_t for the partial derivative with respect to time. The chain rule (14) for a function $f\colon \Omega \times (a, b) \to \mathbb{R}$ and $\boldsymbol{\psi}\colon (a, b) \to \Omega$ with $n = d + 1$ reads

$$\frac{\mathrm{d}}{\mathrm{d}t} f(\boldsymbol{\psi}(t), t) = \partial_t f\big|_{\boldsymbol{x}=\boldsymbol{\psi}(t)} + \frac{\mathrm{d}\boldsymbol{\psi}(t)}{\mathrm{d}t} \cdot \boldsymbol{\nabla} f\big|_{\boldsymbol{x}=\boldsymbol{\psi}(t)}\,. \tag{17}$$

The first term on the right records the change of f coming directly from the time dependence of f, while the second term records the changes from moving along the curve $\boldsymbol{\psi}$. This form of the chain rule arises from (16) by setting $U = \Omega \times (a, b)$ and $\boldsymbol{\phi}(t) = (\boldsymbol{\psi}(t), t)$ so that $\mathrm{d}\boldsymbol{\phi}(t)/\mathrm{d}t = (\mathrm{d}\psi_1(t)/\mathrm{d}t, \ldots, \mathrm{d}\psi_d(t)/\mathrm{d}t, 1)$ and the vector of partial derivatives of f reads $(\partial_1 f, \ldots, \partial_d f, \partial_t f) = (\boldsymbol{\nabla} f, \partial_t f)$.

A.2 Source Strength and the Divergence of a Vector Field

Given a vector field $\boldsymbol{u}$, we measure its "source strength" as follows. For a given sub-volume, for instance a small box Q with boundary S, we define the

flux of $\boldsymbol{u}$ through S as the surface integral

$$\mathrm{Fl} = \int_S \boldsymbol{u} \cdot \mathrm{d}\boldsymbol{A}\,. \tag{18}$$

This integral expresses that we are summing up the component of $\boldsymbol{u}$ which is perpendicular to the boundary S. The flux measures the net volume of fluid crossing S per unit time. Note that the component of $\boldsymbol{u}$ which is parallel to the boundary does not contribute to the flux in or out of the box.

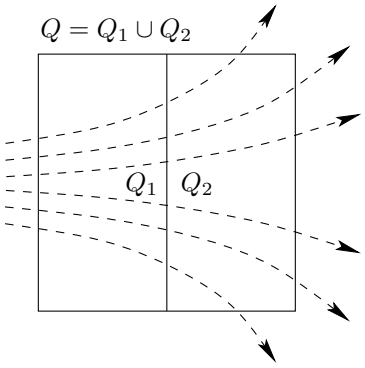

If Q is subdivided into two subelements of volume, say Q_1 and Q_2, then the flux out of Q equals the sum of the fluxes out of Q_1 and out of Q_2, as the contributions on the common boundary cancel. By further repeated subdivision, we can localize the contributions to the flux which are generated by smaller and smaller sub-volumes. Finally, we define the *divergence* of $\boldsymbol{u}$ at $\boldsymbol{x}$, written $\operatorname{div} \boldsymbol{u}$, as the flux out of Q divided by the volume of Q, in the limit of smaller and smaller volume elements Q. The divergence measures how much flux is produced per volume, and this is the "source density" or "source strength". An immediate consequence of this definition is that the flux out of Q equals the volume integral of the source strength over Q, symbolically written as

$$\int_S \boldsymbol{u} \cdot \mathrm{d}\boldsymbol{A} = \int_Q \operatorname{div} \boldsymbol{u}\, \mathrm{d}\boldsymbol{x}\,, \tag{19}$$

where S denotes the surface of Q. This expression is usually referred to as *Gauss' divergence theorem*. A simple calculation reveals that

$$\operatorname{div} \boldsymbol{u} = \partial_1 u_1 + \cdots + \partial_n u_n\,, \tag{20}$$

which can be written symbolically as $\boldsymbol{\nabla} \cdot \boldsymbol{u}$. (Usually, this equation is used as the definition of the divergence; then one needs to prove Gauss' theorem (19). Here, we have essentially taken (19) as a definition, and it is (20) that needs proof.)

The Gauss theorem implies, in particular, that when $\operatorname{div} \boldsymbol{u}(\boldsymbol{x}) > 0$, more fluid comes out of a small box around $\boldsymbol{x}$ than flows in, and there is a "source" at $\boldsymbol{x}$ — the fluid expands. Correspondingly, if $\operatorname{div} \boldsymbol{u}(\boldsymbol{x}) < 0$, then more fluid comes in than flows out — the fluid contracts. If $\operatorname{div} \boldsymbol{u} = 0$ at all points, then inflow balances outflow everywhere and the flow preserves volume.

A.3 Deviations from Averages and the Laplace Operator

The *Laplacian* Δ of a real-valued function f in n variables measures how much the value of f at a point $\boldsymbol{x}$ differs from the average of f on small spheres around $\boldsymbol{x}$: let $S_\varepsilon(\boldsymbol{x})$ denote the sphere of radius ε centered at $\boldsymbol{x}$ and let $\mathrm{Av}(f, S_\varepsilon(\boldsymbol{x}))$ denote the average value of f on this sphere. We then define

$$\Delta f = 2n \lim_{\varepsilon \to 0} \frac{\mathrm{Av}(f, S_\varepsilon(\boldsymbol{x})) - f(\boldsymbol{x})}{\varepsilon^2} \,. \tag{21}$$

An intricate computation based on Gauss' theorem (19) shows that the Laplacian is the differential operator

$$\Delta f = \partial_1 \partial_1 f + \cdots + \partial_n \partial_n f \,, \tag{22}$$

which can be written symbolically as $\boldsymbol{\nabla} \cdot \boldsymbol{\nabla} f$. Applied to a vector field, the Laplacian acts on each component separately, i.e., $\Delta \boldsymbol{u} = (\Delta u_1, \ldots, \Delta u_n)$.

To motivate the equivalence of (21) and (22), consider an affinely linear function $f(x) = ax + b$ in one variable; then $\mathrm{d}^2 f / \mathrm{d}x^2 = 0$ and $f(x) = (f(x-\varepsilon) + f(x+\varepsilon))/2$, so $f(x)$ equals the average of all values at distance ε from x; we rewrite this as $f(x+\varepsilon) + f(x-\varepsilon) - 2f(x) = 0$. This is of course not so for non-linear f, but we always have

$$\frac{\mathrm{d}^2 f}{\mathrm{d}x^2} = \lim_{\varepsilon \to 0} \frac{f(x+\varepsilon) + f(x-\varepsilon) - 2f(x)}{\varepsilon^2} \,, \tag{23}$$

the expression for the one-dimensional Laplacian.

A.4 Circulation and the Curl of a Vector Field

Our final differential operator, the curl, is most easily introduced for $n = 3$. There is, however, the beautiful more abstract framework of "differential forms" in which Gauss' theorem (19) and Stokes' theorem below take a simple common form.

Let $C \subset \mathbb{R}^3$ denote a smooth curve, parametrized as $\boldsymbol{s} \colon [a, b] \to C$. The curve is called *closed* if $s(a) = s(b)$, and we assume that the parametrization is traversing the curve once. The *circulation* of $\boldsymbol{u}$ along C is then defined by

$$\oint_C \boldsymbol{u} \cdot \mathrm{d}\boldsymbol{s} = \int_a^b \boldsymbol{u}(\boldsymbol{s}(r)) \cdot \boldsymbol{s}'(r) \, \mathrm{d}r \,. \tag{24}$$

(The small circle in the integral sign indicates that the curve of integration is closed.) The line integral can be thought of as summing up the components of $\boldsymbol{u}$ which are tangential to the curve; it is easy to show that it is independent of the choice of parametrization. It measures the amount of spinning of the flow along the curve C. For instance, water flow around the drain of a water basin often develops a strong circulation around the drain.

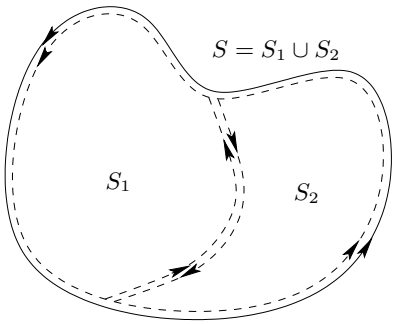

Suppose there is a piece of a surface, say S, for which C is the boundary. The circulation in (24) is found by going once around S. How does the total circulation change if we subdivide S into two subsurfaces S_1 and S_2? When computing the circulation around S_1 and S_2 separately, their common boundary curve is traversed twice, but in opposite direction. The corresponding contributions to the total circulation thus cancel in the sum, and only the contribution from the boundary of S remains. Again, we can ask which part of the surface is responsible for producing circulation by further subdividing S. As the area of the subdivisions tends to zero, the surfaces look more and more like planes, so that it suffices to look at the limit circulation per unit area for planar surface elements. This limit circulation per unit area is called the *curl* of $\boldsymbol{u}$ at point $\boldsymbol{x}$, and is written $\operatorname{curl} \boldsymbol{u}$. It is a vector whose component in the direction perpendicular to a plane P is the circulation of $\boldsymbol{u}$ around a small surface $S \subset P$ containing $\boldsymbol{x}$, divided by the area of S, in the limit that this area tends to zero. Consequently,

$$\int_S \operatorname{curl} \boldsymbol{u} \cdot \mathrm{d}\boldsymbol{A} = \oint_C \boldsymbol{u} \cdot \mathrm{d}\boldsymbol{s}\,, \tag{25}$$

where we may interpret $\operatorname{curl} \boldsymbol{u}$ as a vector field and the left hand integral as the total flux of $\operatorname{curl} \boldsymbol{u}$ through the surface S. Equation (25) is usually referred to as *Stokes' theorem*. To determine the three vector components of the curl, it is sufficient to compute the limit circulation per unit area in the each of the three coordinate planes. A calculation which we will not reproduce here, but that we encourage our readers to find for themselves, yields

$$\operatorname{curl} \boldsymbol{u} = (\partial_2 u_3 - \partial_3 u_2, \partial_3 u_1 - \partial_1 u_3, \partial_1 u_2 - \partial_2 u_1)\,, \tag{26}$$

which can be written symbolically as the vector product $\boldsymbol{\nabla} \times \boldsymbol{u}$. If $\boldsymbol{u}$ is the velocity field of a fluid, we refer to $\operatorname{curl} \boldsymbol{u}$ as the *vorticity*. Its third component, for instance, measures how much the flow restricted to the (x_1, x_2)-plane rotates about the axis through $\boldsymbol{x}$ in the x_3-direction.

Appendix B. Energy Estimates

In this appendix, we derive simple estimates for smooth solutions of the Navier-Stokes equations which are remarkably close to the best known. We treat only the case of periodic boundary conditions. The main result is the

"energy relation" (32), which expresses that the total kinetic energy is constant for solutions of the Euler equations and strictly decreasing for solutions of the Navier–Stokes equations where friction comes into play. We also indicate how energy estimates can lead to bounds on derivatives, and where the difficulty in establishing better bounds comes from.

B.1 Energy is Non-Increasing

We begin by taking the dot product of the Navier–Stokes momentum equation (6a) with $\boldsymbol{u}$ and integrating over the space domain Ω:

$$\int_\Omega \boldsymbol{u} \cdot \frac{\partial \boldsymbol{u}}{\partial t} \,\mathrm{d}\boldsymbol{x} + \int_\Omega \boldsymbol{u} \cdot (\boldsymbol{u} \cdot \boldsymbol{\nabla} \boldsymbol{u}) \,\mathrm{d}\boldsymbol{x} + \int_\Omega \boldsymbol{u} \cdot \boldsymbol{\nabla} p \,\mathrm{d}\boldsymbol{x} = \nu \int_\Omega \boldsymbol{u} \cdot \Delta \boldsymbol{u} \,\mathrm{d}\boldsymbol{x} \,. \quad (27)$$

Writing

$$|\boldsymbol{u}|^2 = \sum_{i=1}^{d} |u_i|^2 \quad \text{and} \quad |\boldsymbol{\nabla} \boldsymbol{u}|^2 = \sum_{i,j=1}^{d} |\partial_i u_j|^2 \,, \quad (28)$$

recognizing that $\partial |\boldsymbol{u}|^2 / \partial t = 2\, \boldsymbol{u} \cdot \partial \boldsymbol{u} / \partial t$ and $\boldsymbol{u} \cdot \boldsymbol{\nabla} |\boldsymbol{u}|^2 = 2\, \boldsymbol{u} \cdot (\boldsymbol{u} \cdot \boldsymbol{\nabla} \boldsymbol{u})$, and moving the time derivative under the integral, we obtain

$$\frac{1}{2} \frac{\mathrm{d}}{\mathrm{d}t} \int_\Omega |\boldsymbol{u}|^2 \,\mathrm{d}\boldsymbol{x} + \frac{1}{2} \int_\Omega \boldsymbol{u} \cdot \boldsymbol{\nabla} |\boldsymbol{u}|^2 \,\mathrm{d}\boldsymbol{x} + \int_\Omega \boldsymbol{u} \cdot \boldsymbol{\nabla} p \,\mathrm{d}\boldsymbol{x} = \nu \int_\Omega \boldsymbol{u} \cdot \Delta \boldsymbol{u} \,\mathrm{d}\boldsymbol{x} \,. \quad (29)$$

Now, if f is a function and $\boldsymbol{v}$ a vector field, then $\operatorname{div}(f \boldsymbol{v}) = f \operatorname{div} \boldsymbol{v} + \boldsymbol{v} \cdot \boldsymbol{\nabla} f$. Thus, applying Gauss' theorem (19) to $f \boldsymbol{v}$ and noting that the boundary integral on the left of (19) vanishes (because contributions from opposite boundary faces of our periodic domain cancel), we obtain the multi-dimensional "integration by parts" formula

$$\int_\Omega \boldsymbol{v} \cdot \boldsymbol{\nabla} f \,\mathrm{d}\boldsymbol{x} = -\int_\Omega f \operatorname{div} \boldsymbol{v} \,\mathrm{d}\boldsymbol{x} \,. \quad (30)$$

Hence, the second and third terms in (29) vanish altogether: after integrating by parts, the integrands each contain the factor $\operatorname{div} \boldsymbol{u}$, which is zero. Writing $\Delta \boldsymbol{u} = \boldsymbol{\nabla} \cdot \boldsymbol{\nabla} \boldsymbol{u}$ and integrating by parts in the last term of (29), we find

$$\frac{1}{2} \frac{\mathrm{d}}{\mathrm{d}t} \int_\Omega |\boldsymbol{u}|^2 \,\mathrm{d}\boldsymbol{x} = -\nu \int_\Omega |\boldsymbol{\nabla} \boldsymbol{u}|^2 \,\mathrm{d}\boldsymbol{x} \,. \quad (31)$$

Integration with respect to time finally yields the "energy relation"

$$E(t) \equiv \frac{1}{2} \int_\Omega |\boldsymbol{u}(t)|^2 \,\mathrm{d}\boldsymbol{x} = E(0) - \nu \int_0^t \int_\Omega |\boldsymbol{\nabla} \boldsymbol{u}(s)|^2 \,\mathrm{d}\boldsymbol{x} \,\mathrm{d}s \,. \quad (32)$$

Since the integrand in the last term is non-negative, the energy E is non-increasing and the cumulative energy dissipation (11) is bounded by the initial

energy $E(0)$. For the Euler equations where $\nu = 0$, energy is a constant of the motion, but there is no implied bound on the space-time integral of $|\boldsymbol{\nabla u}|^2$.

B.2 Bounds on Derivatives

Let us now consider how the energy relation may control derivatives of $\boldsymbol{u}$. The essential difficulty lies in getting control of, in particular, the integral of $|\boldsymbol{\nabla u}|^2$ over Ω pointwise in time; if this were done, bounds on derivatives of any order would follow by standard arguments. In an attempt to prove the required bound, we take the dot product of (6a) with $\Delta \boldsymbol{u}$ and integrate over the spatial domain as before,

$$\int_\Omega \Delta \boldsymbol{u} \cdot \partial_t \boldsymbol{u} \,\mathrm{d}\boldsymbol{x} + \int_\Omega \Delta \boldsymbol{u} \cdot (\boldsymbol{u} \cdot \boldsymbol{\nabla u}) \,\mathrm{d}\boldsymbol{x} + \int_\Omega \Delta \boldsymbol{u} \cdot \boldsymbol{\nabla} p \,\mathrm{d}\boldsymbol{x} = \nu \int_\Omega |\Delta \boldsymbol{u}|^2 \,\mathrm{d}\boldsymbol{x} \,. \quad (33)$$

Integration by parts readily identifies the first term as the time derivative of $|\boldsymbol{\nabla u}|^2$ and lets the pressure contribution vanish as before. However, the second term — containing the contribution from the Navier–Stokes nonlinearity — does not vanish. After a short computation, we obtain

$$\frac{1}{2}\frac{\mathrm{d}}{\mathrm{d}t} \int_\Omega |\boldsymbol{\nabla u}|^2 \,\mathrm{d}\boldsymbol{x} + \sum_{i,j,k=1}^{d} \int_\Omega \partial_i u_j \, \partial_i u_k \, \partial_k u_j \,\mathrm{d}\boldsymbol{x} = -\nu \int_\Omega |\Delta \boldsymbol{u}|^2 \,\mathrm{d}\boldsymbol{x} \,. \quad (34)$$

The second term looks complicated and does not have a definite sign. Simplemindedly, we bound each gradient by its Euclidean length: when $\nu > 0$,

$$\begin{aligned} \left| \sum_{i,j,k=1}^{d} \int_\Omega \partial_i u_j \, \partial_i u_k \, \partial_k u_j \,\mathrm{d}\boldsymbol{x} \right| &\le \int_\Omega |\boldsymbol{\nabla u}|^3 \,\mathrm{d}\boldsymbol{x} \\ &\le c_1 \left(\int_\Omega |\Delta \boldsymbol{u}|^2 \,\mathrm{d}\boldsymbol{x} \right)^{\frac{d}{4}} \left(\int_\Omega |\boldsymbol{\nabla u}|^2 \,\mathrm{d}\boldsymbol{x} \right)^{\frac{6-d}{4}} \\ &\le \nu \int_\Omega |\Delta \boldsymbol{u}|^2 \,\mathrm{d}\boldsymbol{x} + c_2 \left(\int_\Omega |\boldsymbol{\nabla u}|^2 \,\mathrm{d}\boldsymbol{x} \right)^{d} , \quad (35) \end{aligned}$$

where c_1 and $c_2 = c_2(\nu)$ are known positive constants and $d = 2$ or $d = 3$. The proof of the second inequality requires some technical tricks in multivariate integration; the values of the right hand exponents, however, follow from a simple scaling argument which expresses that the inequality preserves physical units. The third inequality is simply a variant of the arithmetic-geometric mean inequality. Altogether,

$$\frac{1}{2}\frac{\mathrm{d}}{\mathrm{d}t} \int_\Omega |\boldsymbol{\nabla u}|^2 \,\mathrm{d}\boldsymbol{x} \le c_2 \left(\int_\Omega |\boldsymbol{\nabla u}|^2 \,\mathrm{d}\boldsymbol{x} \right)^{d} . \quad (36)$$

When $d = 2$, equation (36) can be interpreted as a linear nonautonomous differential inequality: due to the boundedness of the cumulative energy dissipation (11), a standard "integrating factor" argument yields a global bound

on the integral of $|\boldsymbol{\nabla u}|^2$. When $d = 3$, this differential inequality is truly nonlinear so that the implied bound blows up in finite time. In in other words, energy and cumulative energy dissipation are too weak to control the development of fine scales.

The argument can be tweaked to show that when $d = 3$, global solutions exist provided the initial data is sufficiently small, the viscosity ν is sufficiently large, or the initial data is in various ways close to some global regular special situation (as already mentioned in Section 4). Tweaking at this level or looking for more clever choices of function spaces, however, can neither alter the dimensional scaling of the terms in the equation nor the fact that in three dimensions the energy relation provides the strongest known globally controlled quantities. Hence, the greater strength of the nonlinear term relative to dissipation seen in the argument above is invariant under a large class of possible approaches.

The place where we butchered the argument is the first inequality in (35) where all of the three-dimensional geometry of the flow was thrown out. This geometry, or equivalently the geometry of vortex stretching, is arguably the key to progress. Yet, it remains poorly understood because it does not map easily into the language of continuity and compactness of mappings between topological vector spaces, and the latter forms the backbone of much of the theory of partial differential equations.

Appendix C. Spectral and Pseudo-Spectral Schemes

In this section, we briefly introduce spectral methods which are often the method of choice for the computational study of turbulence and blowup. Spectral methods rely on the Fourier series (or spectral decomposition) of the fluid fields.

Compared with alternative numerical schemes, spectral methods are fast, accurate, and easy to compare to many mathematical results. The last is because much of the mathematical analysis of partial differential equations uses spectral decompositions at some level. The main drawbacks of spectral methods are that they lose many of their advantages if used for anything except the simplest possible boundary geometries and, more serious in our case, they do not allow refinement if the most intense structures are very localized such as near developing singularities.

Under mild assumptions, the velocity field $\boldsymbol{u}$ has a unique representation in terms of the *Fourier series*

$$\boldsymbol{u}(\boldsymbol{x}, t) = \sum_{\boldsymbol{k} \in \mathbb{Z}^d} \boldsymbol{u}_{\boldsymbol{k}}(t)\, \mathrm{e}^{\mathrm{i}\boldsymbol{k}\cdot\boldsymbol{x}} \tag{37}$$

where, for convenience, we have scaled our box-shaped periodic domain such that $\Omega = [0, 2\pi]^d$. Each of the *Fourier coefficients* $\boldsymbol{u}_{\boldsymbol{k}}$ is a d-dimensional vector of complex numbers; the index $\boldsymbol{k}$ is referred to as the *wavenumber*. By taking the gradient of (37), we see that differentiation of $\boldsymbol{u}$ is equivalent to multiplication by $\mathrm{i}\boldsymbol{k}$ on the Fourier side,

$$\boldsymbol{\nabla} \boldsymbol{u}(\boldsymbol{x}, t) = \sum_{\boldsymbol{k} \in \mathbb{Z}^d} \mathrm{i}\boldsymbol{k}\, \boldsymbol{u}_{\boldsymbol{k}}(t)\, \mathrm{e}^{\mathrm{i}\boldsymbol{k}\cdot\boldsymbol{x}} \,. \tag{38}$$

This observation can be turned into a numerical method by assuming that only the coefficients $\boldsymbol{u}_{\boldsymbol{k}}$ with $|\boldsymbol{k}| < n/2$ for some n are nonzero, so that the Fourier series involves no more than n^d summands. Consequently, the linear terms in (5) and (6) can be represented exactly by algebraic operations on this finite set of coefficients. The first apparent drawback is that a direct evaluation of the nonlinearity in the Fourier representation requires n^{2d} operations compared to n^d for the other terms, which would be prohibitively expensive.

Another problem stemming from the nonlinear term is that upon each new nonlinear evaluation, required for time advancement, the number of nonzero coefficients expands by a factor of 2^d. If these terms become large and cannot be neglected, then the required amount of computer memory will grow exponentially. Physically, this is perfectly reasonable, as it corresponds to the emergence of smaller scale structures as the flow evolves. This is called a *cascade* in the theory of turbulence. Cascades are naturally described in Fourier space, but are difficult to identify in the physical domain.

The inefficiency of calculating the nonlinearity in Fourier space is addressed by using the linear one-to-one correspondence between our set of n^d nonzero Fourier coefficients and the n^d values on equidistant mesh points in the physical domain. Since multiplication is cheap on the physical space mesh, we compute it there. Operations involving derivatives can be done efficiently in Fourier space. And the map between the Fourier representation and the physical space representation can be computed efficiently by the *fast Fourier transform*, or FFT, in just $n^d \ln n$ operations, i.e., we can map back and forth as needed without significant slowdown. Methods that split the operations in this way are known as *pseudo-spectral* codes.

Once the manner of calculating the spatial derivatives and the nonlinear interaction has been established, we have reduced the problem to solving a system of coupled ordinary differential equations. Combinations of well-known algorithms for the numerical solution of ordinary differential equations are then used to propagate the solution forward in time.

Pseudo-spectral approximations must be *dealiased* by setting to zero an appropriate set of the high wavenumber Fourier modes — the details are outside the scope of this discussion — to ensure that the results are mathematically equivalent to a truncation of the Fourier series as indicated earlier. Doing so ensures that quadratic invariants such as the energy in the Euler

equations remain constants of the motion. However, errors still appear at the scale of the mesh spacing, that is in the high wavenumber Fourier coefficients, and in non-quadratic conservation laws such as the circulation — properties which can be monitored to assess the accuracy of a calculation [3, 11, 15].

Ultimately, the only way to ensure accuracy is to apply more resources, that is redo the calculations on finer meshes. In practice, when performing simulations at the limit of available resolution, a clear understanding of the biases of the chosen numerical scheme is as important as an understanding of the properties of the underlying partial differential equation. And often, the mathematical study of the numerical scheme is an interesting and worthwhile undertaking in its own right.

References

[1] J. Thomas Beale, Tosio Kato, and Andrew J. Majda, *Remarks on the breakdown of smooth solutions for the* 3*-D Euler equations*. Communications in Mathematical Physics **94** (1984), 61–66.

[2] Claude Bardos and Edriss S. Titi, *Euler equations for incompressible ideal fluids*. Russian Mathematical Surveys **62** (2007), 409–451.

[3] Miguel D. Bustamante and Robert M. Kerr, *3D Euler about a 2D symmetry plane*. Physica D: Nonlinear Phenomena **237** (2008), 1912–1920.

[4] Marco Cannone and Susan Friedlander, *Navier: blow-up and collapse*. Notices of the American Mathematical Society **50** (2003), 7–13.

[5] Peter Constantin, *On the Euler equations of incompressible fluids*. Bulletin of the American Mathematical Society **44** (2007), 603–621.

[6] Charles R. Doering, *The 3D Navier–Stokes problem*. Annual Review of Fluid Mechanics **41** (2009), 109–128.

[7] Gregory L. Eyink, *Dissipative anomalies in singular Euler flows*. Physica D: Nonlinear Phenomena **237** (2008), 1956–1968.

[8] Charles L. Fefferman, *Existence & Smoothness of the Navier–Stokes Equation*. Clay Mathematics Institute, 2000; `http://www.claymath.org/millennium/Navier-Stokes_Equations/navierstokes.pdf`.

[9] Ciprian Foias, Oscar P. Manley, Ricardo M. S. Rosa, and Roger M. Temam, *Navier–Stokes Equations and Turbulence*. Cambridge University Press, Cambridge, 2001.

[10] John D. Gibbon, *The three-dimensional Euler equations: Where do we stand?* Physica D: Nonlinear Phenomena **237** (2008), 1894–1904.

[11] Tobias Grafke, Holger Homann, Jürgen Dreher, and Rainer Grauer, *Numerical simulations of possible finite time singularities in the incompressible Euler equations: comparison of numerical methods*. Physica D: Nonlinear Phenomena **237** (2008), 1932–1936.

[12] John G. Heywood, *Remarks on the possible global regularity of solutions of the three-dimensional Navier–Stokes equations*. In: *Progress in Theoretical and Computational Fluid Mechanics*, Giovanni P. Galdi, Josef Málek, and Jindřich Nečas (editors), Paseky 1993, Pitman Research Notes in Mathematics Series Vol. 308, Pitman, London, 1994, 1–32.

[13] Thomas Y. Hou and Ruo Li, *Dynamic depletion of vortex stretching and nonblowup of the 3-D incompressible Euler equations*. Journal of Nonlinear Science **16** (2006), 639–664.

[14] Robert M. Kerr, *Evidence for a singularity of the three-dimensional, incompressible Euler equations*. Physics of Fluids A **5** (1993), 1725–1746.
[15] Robert M. Kerr, *Computational Euler history*. Preprint, July 19, 2006, 20 pages; `http://arxiv.org/abs/physics/0607148v2`.
[16] Andrew J. Majda and Andrea L. Bertozzi, *Vorticity and Incompressible Flow*. Cambridge University Press, Cambridge, 2002.
[17] Terence Tao, *Why global regularity for Navier–Stokes is hard*, 2007; `http://terrytao.wordpress.com/2007/03/18/why-global-regularity-for-navier-stokes-is-hard/`.
[18] Lloyd N. Trefethen, *Ten digit problems*. In: *An Invitation to Mathematics: From Competitions to Research* (this volume).